



## ORIGINAL ARTICLE

# Photodynamic cytotoxic and antibacterial evaluation of *Tecoma stans* and *Narcissus tazetta* mediated silver nanoparticles



Hina Tariq<sup>a</sup>, Muhammad Rafi<sup>b</sup>, Muhammad Imran Amirzada<sup>a</sup>,  
Syed Aun Muhammad<sup>c</sup>, Muhammad Arfat Yameen<sup>a</sup>, Abdul Mannan<sup>a</sup>,  
Tariq Ismail<sup>a</sup>, Irum Shahzadi<sup>d</sup>, Ghulam Murtaza<sup>e,\*</sup>, Nighat Fatima<sup>a,\*</sup>

<sup>a</sup> Department of Pharmacy, COMSATS University Islamabad, Abbottabad Campus 22060, Pakistan

<sup>b</sup> Photomedicine Research Laboratory, Department of Physics and Applied Mathematics, Pakistan Institute of Engineering and Applied Sciences, Nilore, Islamabad, Pakistan

<sup>c</sup> Institute of Molecular Biology and Biotechnology, Bahauddin Zakariya University, Multan, Pakistan

<sup>d</sup> Department of Biotechnology, COMSATS University Islamabad, Abbottabad Campus 22060, Pakistan

<sup>e</sup> Department of Pharmacy, COMSATS University Islamabad, Lahore Campus 54000, Lahore, Pakistan

Received 17 October 2021; accepted 13 December 2021

Available online 17 December 2021

## KEYWORDS

Antioxidant;  
Antibacterial;  
Anticancer;  
Photodynamic therapy;  
Green synthesis

**Abstract** Nanobiotechnology is the intersection of nanotechnology and biology, where nano systems are applied to help study biological systems. There is a growing interest of researchers in the application of nanotechnology in improving the efficacy of photodynamic therapy. In this study, the antioxidant, photodynamic, anticancer, and antibacterial potential of plant extracts and silver nanoparticles (AgNPs) were investigated. In order to synthesize AgNPs, 10 g of dried powder of *Tecoma stans* and *Narcissus tazetta* was boiled in deionized water (100 ml) and mixed with aqueous solution of silver metals, resulting in the formation of AgNPs. The synthesized AgNPs were spherical having size in a range of 15–100 nm. The application of extract (50 µl) and AgNPs to rhabdomyosarcoma cell line showed a decreased cell viability (%). Photodynamic study revealed an improvement in photosensitizer efficacy on introducing AgNPs. Both plant extracts and AgNPs had significant effect against methicillin resistant *Staphylococcus aureus* (MRSA) as well as sensitive *Staphylococcus aureus* with minimum inhibitory concentration (MIC) values of AgNPs lower (32–256 µg/ml) than the plant extracts. According to the current findings, these AgNPs have an enhancing effect on the photodynamic cytotoxic potential of plant extracts. Because of biological efficacy,

\* Corresponding authors.

E-mail addresses: [gmdogar@cuilahore.edu.pk](mailto:gmdogar@cuilahore.edu.pk) (G. Murtaza), [nighatfatimamr1@gmail.com](mailto:nighatfatimamr1@gmail.com) (N. Fatima).

Peer review under responsibility of King Saud University.



these AgNPs may play a crucial role in determining therapeutic potential of *Tecoma stans* and *Narcissus tazetta*.

© 2021 The Authors. Published by Elsevier B.V. on behalf of King Saud University. This is an open access article under the CC BY-NC-ND license (<http://creativecommons.org/licenses/by-nc-nd/4.0/>).

## 1. Introduction

Clinical applications of photodynamic therapy (PDT) is a two-stage modality for the treatment of malignant and non-malignant tumors. PDT involves the combination of photosensitizers (PS) along with light of a specific wavelength in the presence of molecular or tissue oxygen to elicit its pharmacological response. PS is specifically concentrated in the malignant tissue. Through the provision of oxygen along with light projected on the lesion, PS produces reactive oxygen species (ROS) that ultimately cause cell destruction (Dube et al., 2018). Due to specificity and selectivity, PDT is particularly important in cancer therapy (Ogawara and Higaki, 2017). However, more recently, nanotechnology combined with PDT has gained tremendous importance. Nanoparticles alone or with different photosensitizers can be used for targeted drug delivery against various ailments generally and against cancer, specifically (Tang et al., 2017).

Nanotechnology has led to innovative technologies which have found numerous useful applications in numerous fields, including (but not limited to) medical physics and catalysis (Luna et al., 2015). These nanomaterials are unique in size and render them superior and indispensable in different therapeutic fields (Mafiz et al., 2015). In creating novel diagnostic and analytical methods for the detection of clinically significant substances, combining synthetic macromolecules and biomolecular identification units are promising (Samberg et al., 2011). Several methods have been documented for the synthesis of nanoparticles. Physical methods include ablation, high energy irradiation, planetary ball mill, vibrating ball mill and low, high energy ball mill for the synthesis of nanoparticles. Synthetic methods include sol-gel, vapor deposition, spray and laser pyrolysis (Samberg et al., 2011). While chemical and physical techniques favor the production of nanoparticles with suitable characteristics, these techniques are relatively costly and environmentally unsafe (Makwana et al., 2015). Many biological organisms like plant extract biomass and microorganisms could be an alternative material for the production of nanoparticles. The green synthesis of nanoparticles has gained an advantage due to being environmentally friendly and cost-effective (Vinayagam et al., 2017; Varadavenkatesan et al., 2021; Varadavenkatesan et al., 2019). Plant-mediated production of nanoparticles has revealed applications in numerous fields, including biomedical, food packaging and wound healing (Vinayagam et al., 2017). Nanoparticles are stabilized by various phytochemicals such as saponins, carbohydrates, steroids and flavonoids under the effect of their capping and reducing potential (Varadavenkatesan et al., 2021). Silver nanoparticles (AgNPs) have distinctive features. For instance, AgNPs are easy to synthesize, have chemical stability, show good conductivity (making it a suitable candidate for the synthesis of AgNPs) (Vinayagam et al., 2017), exhibit catalytic and most importantly antimicrobial, anti-viral and anticancer activities (Varadavenkatesan et al., 2019). An ele-

vated surface area of AgNPs, excellent biocompatibility, easy surface modification and appropriate cell penetration, make AgNPs effective in application of cell imaging (Vinayagam et al., 2017) and drug delivery (Varadavenkatesan et al., 2019). The literature study describes the successful synthesis of AgNPs through several physicochemical ways. However, most of these approaches involve the use of costly and corrosive chemicals, which can significantly enhance the cost of procedures and adversely affect the ecosystem. These disadvantages could be avoided by using cheap and environment-friendly approaches such as the application of botanical extracts in organic AgNPs synthesis (Luna et al., 2015).

Researchers have brought significant revolution in the field of photodynamic therapy by developing AgNPs through green synthesis, thus two plants *Tecoma stans* (*T. stans*) and *Narcissus tazetta* (*N. tazetta*) were chosen for their synthesis. *T. stans* is a garden ornamental having a variety of therapeutic applications, for example, as an antioxidant, antiproliferative, wound healing, cytotoxic, and antimicrobial agent (Mariselvam et al., 2014). *N. tazetta* is a perennial plant possessing antimicrobial, antiviral, antitumor and anti-hypertensive activities (Nabikhan et al., 2010). Both plants are rich in polyphenols (Mariselvam et al., 2014; Nabikhan et al., 2010). According to our best knowledge, no study describes AgNPs synthesis using the extracts of these plants. In the current work, we synthesized the AgNPs based on green chemistry. Our framework comprehensively describes AgNPs synthesis using *T. stans* and *N. tazetta* plant extracts as reducing agents. These particles were characterized by UV-spectrophotometer, FTIR, and SEM. We observed the potential activities of these nanoparticles. The synthesized AgNPs were investigated for their photodynamic cytotoxicity, antibacterial potential, and antioxidant activity.

## 2. Materials and methods

### 2.1. Collecting and identifying the plant specimens

Dr. Abdul Nazir from COMSATS University Islamabad helped to identify the freshly collected plants. The plants were identified as *Tecoma stans* and *Narcissus tazetta*. Plant material was shade-dried and then powdered with the help of grinder.

### 2.2. Extract preparation

After conducting methanolic maceration of the powdered plant material with agitation for 3 days at room temperature, solvent layer was removed from solid plant material by using Whatman filter paper. After filtration, the obtained material was processed through rotary evaporator to get a concentrated filtrate. The obtained extract was then stored at 4 °C till further analysis.

### 2.3. Production of silver nanoparticles

In order to synthesize AgNPs, 10 g of dried powder of *Tecoma stans* and *Narcissus tazetta* was boiled in deionized water (100 ml) (Ahmed et al., 2016). Measured volume of the dry powder infusion was mixed with 1, 5 and 10 mM aqueous solution of silver metals. After incubating the reaction mixture at room temperature (25 °C) for 24 h in the dark, the reaction mixture was observed for color change due to reduction reaction and put on centrifugation at 12,000 rpm for 15 min. As a result, AgNPs pellet was acquired, washed and stored.

### 2.4. Activity testing of extracts and silver nanoparticles

#### 2.4.1. Antibacterial test

The extracts and AgNPs were tested for their antibacterial potential using the well diffusion method (Anburaj et al., 2016). The selected bacterial strains were *Staphylococcus aureus* ATCC# 6538 (*S. aureus*), MRSA 10, and MRSA 11. Results were presented as a diameter of zone of inhibition (mm) and MIC (Vacik et al., 1979).

#### 2.4.2. Antioxidant test

DPPH (2,2-diphenyl-1-picrylhydrazyl) assay was conducted to evaluate the antioxidant potential of extracts and AgNPs (Kaviya and Viswanathan, 2011). The sample (20 µl) and DPPH (180 µl) were added to 96 well-plate. The study involved the use of DMSO and ascorbic acid as negative and positive control, respectively. After taking absorbance at 517 nm using microplate reader, percent scavenging was calculated by using below given formula:

$$\text{Inhibition (\%)} = (1 - A_s/A_c) \times 100$$

Where,  $A_s$  and  $A_c$  are the absorbances of sample and reagent without sample, respectively. IC<sub>50</sub> values were calculated for those samples that showed greater than 50% scavenging potential.

#### 2.4.3. Anticancer test and PDT

MTT (3-(4,5-dimethyl thiazol-2yl)-2,5-diphenyl) assay was used for the determination of anticancer potential of extracts and AgNPs using rhabdomyosarcoma (RDATCC# CCL-136) cell line (Mativandela et al., 2006). Dulbecco's Modified Eagle medium (DMEM; Sterile filtered DMEM (-)L-leucine, (-)L-methionine with 4.5 g/L glucose, 4.0 mM L-glutamine, sodium pyruvate and phenol red) was used for cell culturing. Cell suspension was prepared and 0.2 ml of this cell suspension was added to each well of 96 well plates with density of  $1 \times 10^5$  cells/well and stored at 37 °C in 5% CO<sub>2</sub>. After incubation of plates, medium was replaced by fresh DMEM along with addition of different samples (50 µl), followed by the re-incubation of plates for 2–3 days at 37 °C in 5% CO<sub>2</sub>. From here, the experiment was bifurcated. After incubation, first plate was processed for the removal of medium and washed thrice with PBS. Then, all the wells were treated with MTT solution and the plate was incubated for 200–250 min at 37 °C in 5% carbon dioxide. After incubation, the extracting solution was added and studied using microplate reader at 570 nm after 45 s. Cell Viability (%) was determined using below given formula:

$$\text{Cell Viability (\%)} = (\text{Mean OD}/\text{Control OD}) * 100$$

The samples which showed more than 50% inhibition were further studied for IC<sub>50</sub>.

The second plate was utilized for PDT (Fatima et al., 2016). Photo-sense (aluminum chloride phthalocyanine) and light was shined on respective wells, MTT assay was executed and percentage cell viability and IC<sub>50</sub> values were calculated.

### 2.5. Chemical features of silver nanoparticles

Various techniques were used for the characterization of AgNPs. Their synthesis was confirmed by using UV–visible spectrophotometer (Shimadzu, UV-1280). After diluting with distilled water, sample scanning was conducted in a wavelength range of 300–600 nm and spectra were recorded (Mativandela et al., 2006). FTIR was used for the determination of functional groups of secondary metabolites responsible for reduction of metal to AgNPs. The morphological characteristics of AgNPs were assessed by using SEM (JEOL Japan, SEM JSM5910). The samples were diluted in ethanol and vortexed. Accurately measured suspension (20 µl) was mixed with copper grid and dried. Finally, SEM micrographs of the suspension-loaded copper grids were acquired using SEM equipment.

## 3. Results

### 3.1. Activity testing of extracts and silver nanoparticles

#### 3.1.1. Antibacterial test

Agar well diffusion approach was used to study antibacterial activity against three strains including *S. aureus* (ATCC# 6538), MRSA 10 and MRSA 11. Crude extract of *T. stans* exhibited significantly ( $p < 0.05$ ) highest activity against *S. aureus* (ZOI =  $24.2 \pm 0.9$ ). Crude extract of *T. stans* showed significant ( $p < 0.05$ ) higher activity against all bacterial strains with the maximum value of ZOI of  $24.2 \pm 0.9$  mm against *S. aureus* as compared to the control. The sample of *N. tazetta* was nearly inactive. AgNPs were prepared with varying concentrations of silver nitrate (1, 5 and 10 Mm) and tested for antibacterial potential. Results showed that AgNPs (5 mM) showed ( $p < 0.05$ ) higher antibacterial activity than crude extracts. Maximum ZOI of  $26.2 \pm 0.8$  mm was shown by *T. stans* based AgNPs against *S. aureus* (Table 1). Minimum inhibitory concentration (MIC) was determined against all three strains. MICs for crude extract was very high, ranging between 512 and 1024 µg/ml, but AgNPs showed low MIC values, especially AgNPs prepared from *T. stans* leaves (TSLNp) with values of 16 µg/ml, 32 µg/ml and 32 µg/ml against *S. aureus*, MRSA 10, and MRSA 11, respectively (Table 2).

#### 3.1.2. Antioxidant test

Crude extract of *T. stans* showed significant ( $p < 0.05$ ) activity with more than 80% scavenging potential. Maximum scavenging (%) was shown by *T. stans* leaf extract with a value of 93.5% and IC<sub>50</sub> values of 1.19 µg/ml (Table 3). *N. tazetta* samples exhibited a little antioxidant capability. The scavenging potential of *N. tazetta* based AgNPs ranged from 40 to 51.5%.

**Table 1** Antibacterial activity of plant extract and their metallic nanoparticles.

Samples	Codes	Zones of inhibition (mm)		
		S. aureus	MRSA 10	MRSA 11
Crude extract	TSB	24.2 ± 0.9	23.2 ± 1.1	21.2 ± 0.9
	TSL	15.3 ± 1.2	20.1 ± 1.1	21.2 ± 0.9
	NT	9.6 ± 0.7	9.6 ± 0.7	9.6 ± 0.7
Silver NP's	TSBNp 1 mM	10.4 ± 1.0	7.2 ± 1.0	8.3 ± 1.0
	TSBNp 5 mM	26.2 ± 0.8	25.1 ± 0.9	23.2 ± 1.0
	TSBNp 10 mM	12.5 ± 1.3	15.2 ± 1.3	17.6 ± 1.5
	TSLNp 1 mM	10.5 ± 0.9	7.4 ± 0.9	8.5 ± 0.9
	TSLNp 5 mM	20.2 ± 1.0	25.3 ± 1.0	24.2 ± 1.1
	TSLNp 10 mM	15.3 ± 1.0	16.4 ± 1.2	20.9 ± 1.4
	NTNp 1 mM	9.6 ± 0.7	9.6 ± 0.7	–
	NTNp 5 mM	14.5 ± 0.9	14.3 ± 1.1	15.2 ± 1.2
	NTNp 10 mM	12.3 ± 1.1	13.5 ± 1.1	12.5 ± 1.1
	Standard	22.4 ± 1.0	–	–

Notes: TSB = T. stans branches, TSL = T. stans leaves, NT = N. tazetta, TSBNp = T. stans branches mediated nanoparticles, TSLNp = T. stans leaves mediated nanoparticles, NTNp = N. tazetta mediated nanoparticles, S. aureus, MRSA 10 and 11 = Methicillin resistant S. aureus clinical isolate 10 and MRSA.

**Table 2** MIC of plant extract and their AgNPs.

Samples	Codes	MIC (µg/ml)		
		S. aureus	MRSA 10	MRSA 11
Crude extract	TSB	1024	1024	1024
	TSL	1024	1024	512
	NT	1024	1024	1024
AgNPs	TSBNp	128	256	128
	TSLNp	16	32	32
	NTNp	128	64	128

Notes: TSB = T. stans branches, TSL = T. stans leaves, NT = N. tazetta, TSBNp = T. stans branches mediated nanoparticles, TSLNp = T. stans leaves mediated nanoparticles, NTNp = N. tazetta mediated nanoparticles.

**Table 3** Antioxidant activities of extracts and their AgNPs.

Sample	Codes	Scavenging (%)						IC <sub>50</sub> (µg/ml)
		200 (µg/ml)	100 (µg/ml)	50 (µg/ml)	25 (µg/ml)	12.5 (µg/ml)	6.25 (µg/ml)	
Crude extract	TSB	84.9 ± 0.9	84 ± 1.1	78.8 ± 1.2	70.2 ± 0.7	62.6 ± 0.9	57.3 ± 1.2	2.15 ± 1.0
	TSL	93.5 ± 0.9	90.8 ± 0.9	86.6 ± 0.9	80.8 ± 0.8	75.2 ± 1.1	67.4 ± 0.8	1.19 ± 0.7
	NT	46.9 ± 0.9	30.9 ± 0.7	14.9 ± 0.9	7.9 ± 0.9	7.7 ± 0.9	6.5 ± 0.8	–
AgNPs	TSBNp	50.5 ± 0.9	38.7 ± 1.1	29.0 ± 1.0	22.5 ± 1.0	19.5 ± 0.9	11.5 ± 0.9	211 ± 1.0
	TSLNp	51.5 ± 1.1	45.0 ± 1.1	43.7 ± 1.1	42.7 ± 1.1	37.8 ± 1.1	30.6 ± 0.8	165 ± 1.1
	NTNp	38.8 ± 1.1	30.9 ± 1.0	21.6 ± 1.0	20.2 ± 0.8	19.7 ± 0.9	18.4 ± 0.9	–

Notes: TSB = T. stans branches, TSL = T. stans leaves, NT = N. tazetta, TSBNp = T. stans branches mediated nanoparticles, TSLNp = T. stans leaves mediated nanoparticles, NTNp = N. tazetta mediated nanoparticles.

### 3.1.3. Anticancer test

Extracts of *N. tazetta* showed good cytotoxicity (IC<sub>50</sub> = 16.9 ± 0.6 µg/ml; cell viability (%) = 25.3 ± 1.3), while IC<sub>50</sub> value of its AgNPs was 4.79 ± 1.1 µg/ml. The IC<sub>50</sub> of *T. stans* extract based AgNPs was significantly ( $p > 0.05$ ) lower, i.e. 2.26 ± 0.9 µg/ml (Fig. 1).

### 3.1.4. Photodynamic therapy assay

Both plant extracts and NPs were active in cell line assay and were further used to evaluate their photodynamic potential. It was observed that cell viability was significantly ( $p < 0.05$ ) decreased when these combinations of extract, NPs, drug and photosensitizer were used. Plant extracts and AgNPs were tested at 40 µg/ml. In case of samples of *Tecoma* plant extracts,

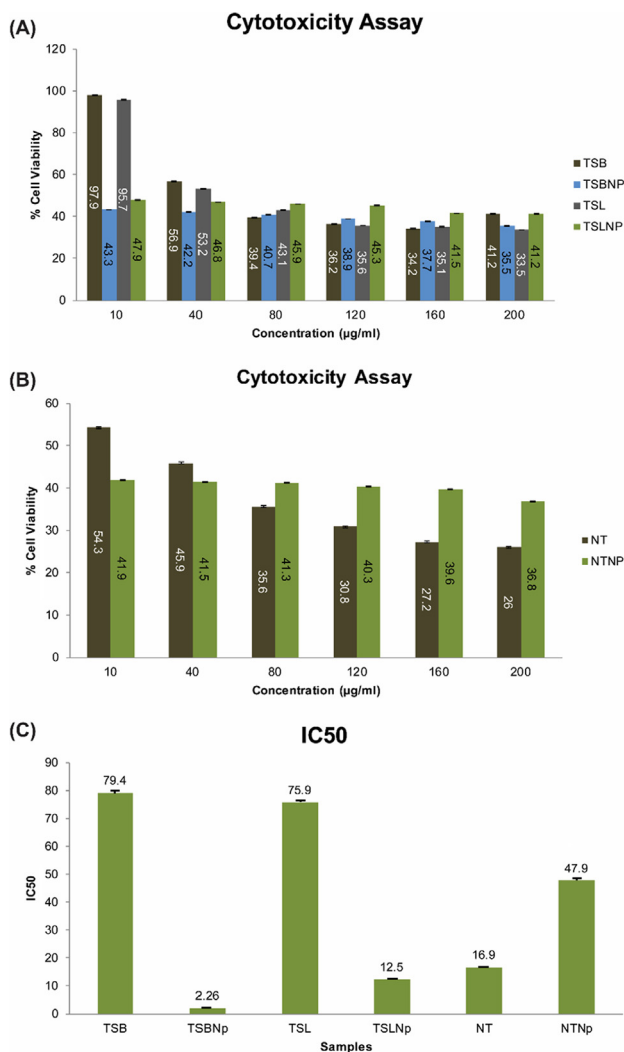


**Fig. 1** Result of anticancer assay of *T. stans* (A), *N. tazetta* (B) and IC<sub>50</sub> values of extracts and nanoparticles (C). (TSB = *T. stans* branches, TSL = *T. stans* leaves, NT = *N. tazetta*, NP's = Nanoparticles).

AgNPs showed % cell viability of 53–57% and 40.8–48.9% respectively, while % cell viability significantly ( $p < 0.05$ ) decreased to 22.4 and 24.9%, respectively, where the combination of plant extract, NPs, drug and photosensitizer was used. The same synergistic behavior was observed with *N. tazetta*

extract and NPs (Table 4). These results were compared to controls.

### 3.2. Characterization of silver nanoparticles

#### 3.2.1. Visual observation and UV–visible spectroscopy

*T. stans* and *N. tazetta* extracts were treated with 1 mM, 5 mM, and 10 mM concentrations of AgNO<sub>3</sub> resulting in the formation of AgNPs, as indicated by the change in solution colour from yellow to brown. UV–vis spectra were recorded by scanning the samples between 300 and 600 nm. Nanoparticles prepared by 5 mM concentration show a sharp peak and lies in the range of 410–420 nm that is characteristic for AgNPs (prepared by chemical reduction). Peaks for 1 mM and 10 mM were not as sharp (Fig. 2).

#### 3.2.2. FTIR spectroscopy

Different peaks were observed in FTIR spectra of AgNPs. Broader peaks were observed at 3295, 3273 and 3220 cm<sup>-1</sup> in the spectra of AgNPs of *Tecoma* branches, leaves and *Narcissus* respectively (Fig. 3). Peaks at 2935, 2897 and 2930 cm<sup>-1</sup> correspond to –C–H stretching vibration in –CH<sub>2</sub> groups. Peaks appear at 1766, 1730, 1633, and 1680 cm<sup>-1</sup> represent C=O stretching vibration. The spectra of *T. stans* leaves showed a broader peak at 3273, 1633 cm<sup>-1</sup>. Other peaks were observed at 2897 and 2370 cm<sup>-1</sup>. Many smaller peaks were also observed at 1730, 1398, 1126, 1033, 976, 948 and 856 cm<sup>-1</sup>. The spectra of branch extract showed a wider peak at 3295 cm<sup>-1</sup>. Small peaks were also observed at 2935, 2853, and 2366 cm<sup>-1</sup>. Narrow peaks were observed at 1766, 1597, 1527, 1386, 1265, 1033 and 826 cm<sup>-1</sup>. Spectra of *N. Tazetta* showed broader peaks at 3220 cm<sup>-1</sup>. Smaller peaks were noted at 1680, 1590, 1539, 1400, 1290, and 1050 cm<sup>-1</sup>. Small narrow peaks were observed at 1290, 1050, 995, 925, and 789 cm<sup>-1</sup> (Fig. 4).

#### 3.2.3. Scanning electron micrograph (SEM) analysis

According to SEM results size of TSBNPs in 20–100 nm while the size range of 10–50 nm was observed in case of TSLNPs. Same behavior was observed by *N. tazetta* sample-based AgNPs with variation in size 30–150 nm.

## 4. Discussion

Photodynamic Therapy (PDT) is a minimally invasive approach for the treatment of skin, esophageal, head and neck,

**Table 4** The synergistic photodynamic anticancer potential of extracts and their AgNPs.

Samples	T. stans	T. stans	N. tazetta
	branches (TB)	leaves (TL)	(N)
Extract (Ext)	57 ± 0.2	53.4 ± 0.07	45 ± 0.09
Ext with photosensitizer (PS)	43.9 ± 0.07	42.9 ± 0.06	39 ± 0.05
Ext. with drug (D)	41.5 ± 0.15	39.7 ± 0.12	36.2 ± 0.05
Nanoparticles NPs	40.8 ± 0.07	48.9 ± 0.09	41.86 ± 0.1
NPs with photosensitizer (PS)	38.3 ± 0.1	43.97 ± 0.04	39 ± 0.07
NPs with drug (D)	37.98 ± 0.12	41.8 ± 0.11	38.6 ± 0.1
Ext. + NPs + PS + D	22.4 ± 0.15	24.9 ± 0.07	27.06 ± 0.04

Controls; Photosensitizer (PS); 45.7%, Doxorubicin (D); 45.2%, Doxorubicin (D) + PS; 65.3%.

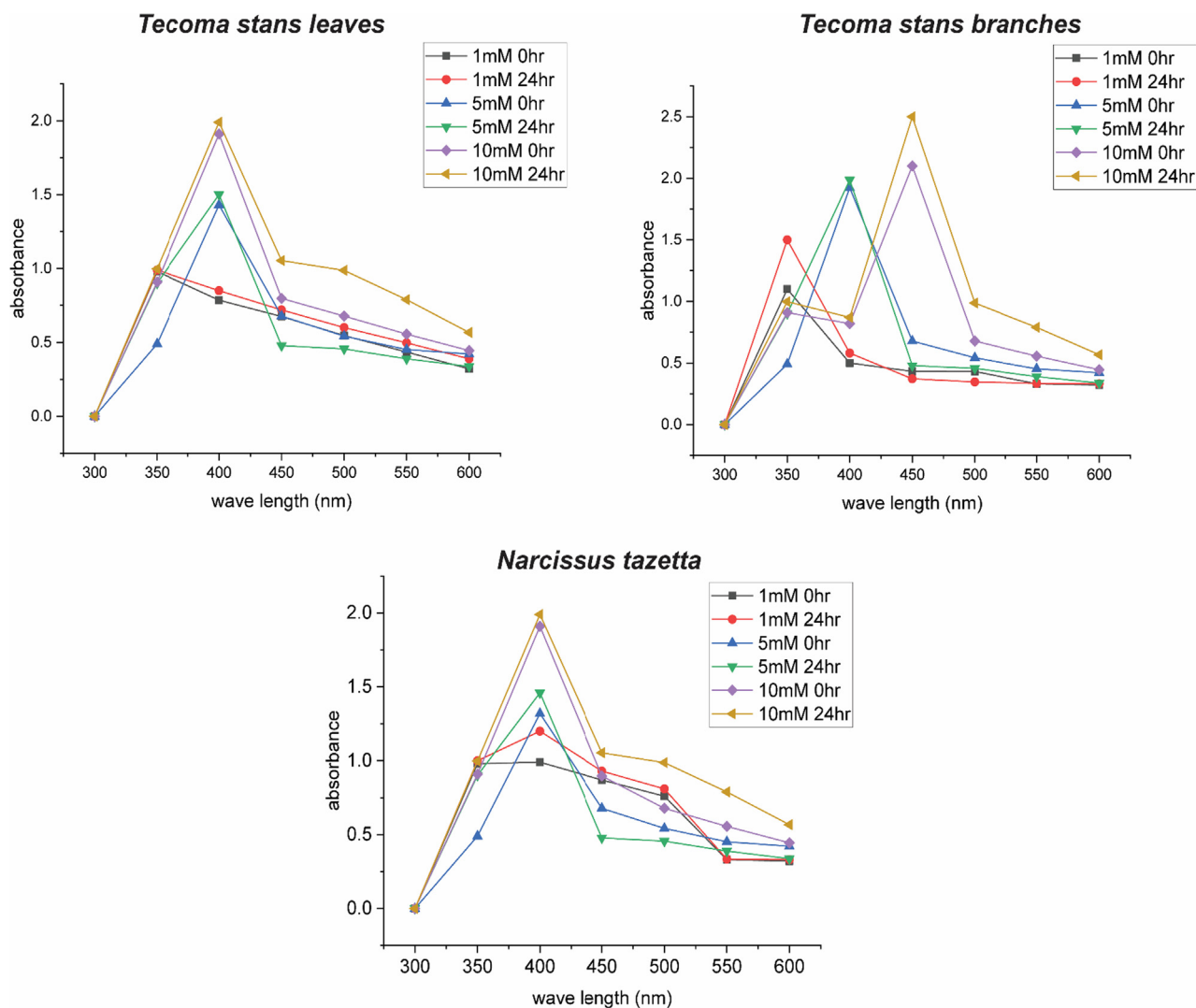


**Fig. 2** UV spectra of *T. stans* and *N. tazetta* nanoparticles.

lung, and bladder cancers with excellent therapeutic efficacy and low side effects (Ogawara and Higaki, 2017). Green nanotechnology is the most advanced field to improve the efficacy of natural products. In this study, two chosen plants and their AgNPs were studied in to determine their biological and pharmacological potential.

#### 4.1. Activity testing of extract and silver nanoparticles

##### 4.1.1. Antibacterial test

Three bacterial strains, *S. aureus* (ATCC# 6538), MRSA 10 and MRSA 11 were used to evaluate antibacterial potential of samples. MRSA 10 and 11 were resistant strains. As compared to the controls, sample of *T. stans* showed significantly ( $p < 0.05$ ) high activity against all selected bacterial strains, while the maximum ZOI ( $24.2 \pm 0.9$  mm) was noted against *S. aureus*. Sample of *N. tazetta* was almost inactive. These results support the previous findings (Masood et al., 2013). AgNPs were synthesized by using silver nitrate (1, 5 and 10 Mm) and tested for antibacterial potential. It was observed

that AgNPs (5 mM) showed significantly ( $p < 0.05$ ) higher antibacterial activity than crude extracts and these AgNPs were selected for further studies. These results support the previous findings as documented by Ravishakar et al., who found that AgNPs showed strong antibacterial activities (Hammad Aziz et al., 2016). MIC values for crude extract were significantly ( $p < 0.05$ ) high, ranging between 256 and 1024  $\mu\text{g}/\text{ml}$ , but AgNPs showed significantly ( $p < 0.05$ ) low MIC values, especially AgNPs prepared from *T. stans* leaves (TSLNp). The MIC of AgNPs synthesized from extract was significantly ( $p < 0.05$ ) decreased due to decreased particle size and large surface area, which led to enhanced cell permeability and damage of bacterial pathogens (Govindappa et al., 2011).

##### 4.1.2. Antioxidant assay (DPPH free radical scavenging activity)

Antioxidants scavenge free radicals and protect the cells against oxidative stress (Fatima et al., 2016). Extract of *T. stans* showed more than 80% scavenging. Leaf extract showed maximum scavenging (%) with a value of 93.5% and IC<sub>50</sub> val-

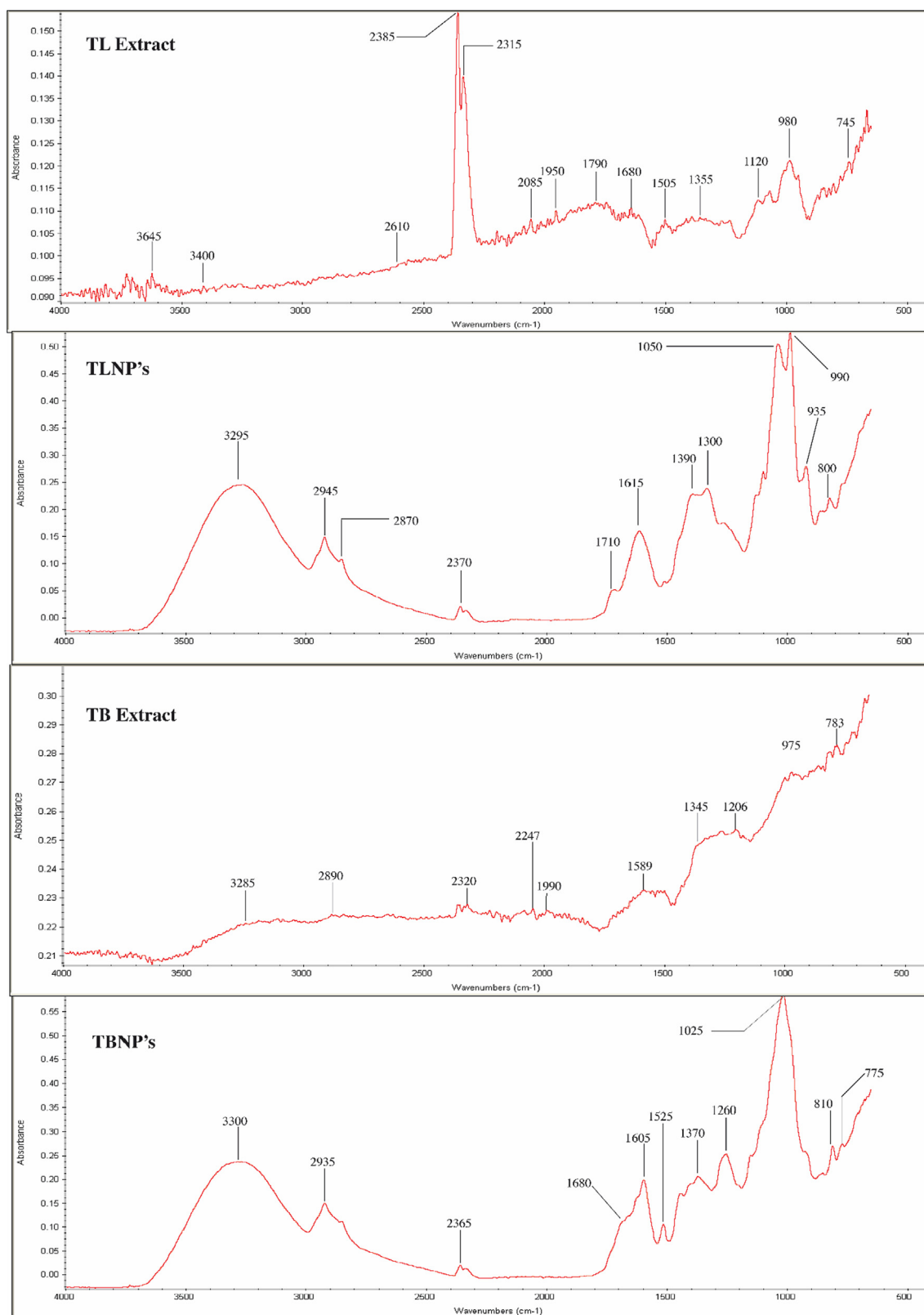


**Fig. 3** FTIR spectra of *T. stans* leaves (TL) and its branches (TB) and nanoparticles.

ues of 1.19  $\mu\text{g/ml}$  (Table 4). These finding correlated with previous reports that flowers and fruits of *T. stans* showed antioxidant potential due to presence of alkaloids and flavone glycosides (Mariselvam et al., 2014). Samples of *N. tazetta*

showed low antioxidant potential. These results support the previous findings about antioxidant potential of this plant. AgNPs of this plant exhibited a moderate scavenging potential (40–51.5%).

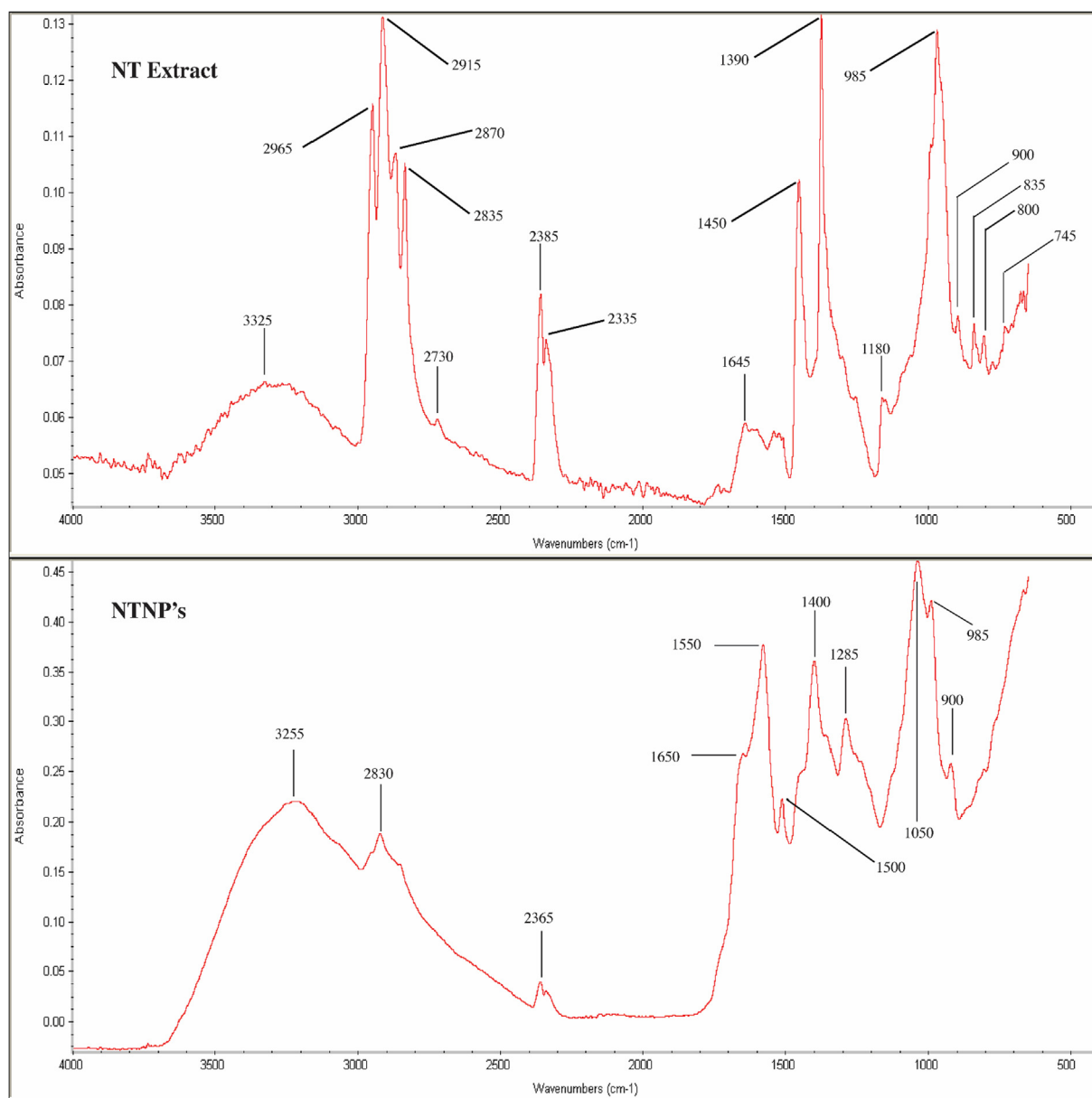


**Fig. 4** FTIR spectra of *N. tazetta* extract and nanoparticles.

#### 4.1.3. Anticancer assay

MTT assay was done to reveal the anticancer potential. In this assay, extracts of *N. tazetta* showed good anticancer activity ( $IC_{50}$  value of  $16.9 \pm 0.6 \mu\text{g/ml}$ ). However, in case of AgNPs, samples of *T. stans* branches showed lower  $IC_{50}$  value of  $2.26 \pm 0.9 \mu\text{g/ml}$ , followed by *N. tazetta* with a value of  $47.9 \pm 1.1 \mu\text{g/ml}$  (Fig. 1C). Both, the methanolic extracts and AgNPs of respective parts showed a dose-dependent decrease in cell viability (%). This trend was in accordance with previous studies (Fu et al., 2016).

#### 4.1.4. Photodynamic therapy

Different combinations of plant extracts and their AgNPs were used to assess photodynamic potential of samples. *Tecoma* plant extracts and AgNPs showed % cell viability of 53–57% and 40.8–48.9% respectively. The percentage cell viability decreased significantly ( $p < 0.05$ ) to 22.4 and 24.9% respec-

tively when combination of plant extract, NPs, drug and photosensitizer was used. Same synergistic behavior was observed with *N. tazetta* extract and NPs. Both extracts and AgNPs were capable of dose and exposure time dependent phototoxicity for rhabdomyosarcoma cell line. This trend was in accordance with the previous studies (Fatima et al., 2016). This is first report about PDT effects of extracts and AgNPs of selected plants.

## 4.2. Characterization of silver nanoparticles

### 4.2.1. Visual observation and UV-visible spectroscopy

The synthesis of AgNPs from plants is considered as an important method due to its potential activities in various studies (Ahmed et al., 2016). *T. stans* and *N. tazetta* extracts were exposed to metal ions ( $\text{AgNO}_3$ ; 1 mM, 5 mM and 10 mM), and the formation of AgNPs was confirmed by color change

i.e., from yellow to brown, due to surface plasmon resonance phenomena. It is also reported by various scientists that biosynthesis may be affected by metal concentration and quantity of plant extract in the reaction medium, which can change the shapes and sizes of AgNPs (Mehrotra et al., 2017). According to UV–vis spectra of the samples recorded between 300 and 600 nm. AgNPs prepared by 5 mM concentration show a sharp peak that lies in the range of 410–420 nm a diagnostic peak indicative of AgNPs (prepared by chemical reduction). Peak intensities give an idea of the size of AgNPs formed (Liu et al., 2006). It should be noted that the UV absorption peak at 440 nm indicates the formation of larger AgNPs (Jain et al., 2009). It is reported previously that AgNPs are formed and stabilized by phenolics, amino acids, carboxylic acids, alkaloids and proteins which are important secondary metabolites (Varadavenkatesan et al., 2021).

#### 4.2.2. Fourier transform infrared spectroscopy (FTIR)

The FTIR spectra indicated the presence of stretching vibration for –OH (alcohol and phenolic), C=O, C–O– (acid), CH, C=C (aromatic system), C–O–(alcohol) and C–N bonds, as well as the functional group which might belong to phenolic and flavonoid compounds present at the surface of the most active NPs. Broader peaks were observed at 3295, 3273 and 3220  $\text{cm}^{-1}$  in spectra of AgNPs of *Tecoma* branches, leaves and *Narcissus* respectively. Peaks at 2935, 2897 and 2930  $\text{cm}^{-1}$  correspond to –C–H stretching vibration in –CH<sub>2</sub> groups. Peaks appear between 1630 and 1766  $\text{cm}^{-1}$  represent the C=O stretching vibration. The flavonoids and phenolic compounds present in the crude extracts are powerful reducing agents which play a significant role in the formation of NPs by the reduction of silver ions. It has already been reported that flavonoids and phenolic compounds present in plant extracts can play a dual function of reducing and capping during NP formation. These findings correlate with previous reports (Ali et al., 2016). Size variation of AgNPs was determined by SEM. AgNPs of *Tecoma* branches showed size of 20–100 nm, while the size of AgNPs from leaf extract was found between 10 and 50 nm. The same behavior was observed by *N. tazetta* sample-based AgNPs. Shape of AgNPs is known for its considerable change in optical and electronic properties. Many researchers have reported the size variation of the green synthesized AgNPs (Ali et al., 2016).

## 5. Conclusion

The present work was focused on the synthesis of AgNPs using *T. stans* and *N. tazetta* plants to determine their biological therapeutic potential. Biologically synthesized AgNPs showed potent antibacterial, antioxidant and photodynamic cytotoxic activities. Green synthesis of AgNPs and their biological therapeutic potential, such as photodynamic anticancer activities against the rhabdomyosarcoma cancer cell line, is reported here in for the first time, further indicating that plants can be used as potential source for drug discovery.

## Declaration of Competing Interest

The authors declare that they have no known competing financial interests or personal relationships that could have appeared to influence the work reported in this paper.

## Acknowledgments

Current work is funded by CIIT Project No. 16-01/CRGP/CIIT/ATD/16/1182.

## References

- Ahmed, S., Ahmad, M., Swami, B.L., Ikram, S., 2016. A review on plants extracts mediated synthesis of silver nanoparticles for antimicrobial application: a green expertise. *J. Adv. Res.* 7, 17–28.
- Ali, M., Bosung, K., Belfield, D.K., Norman, D., Brennan, M., Ali, S. G., 2016. Green synthesis and characterization of silver nanoparticles using *Artemisia absinthium* aqueous extract, A comprehensive study. *Mater. Sci. Eng. C* 58, 359–365.
- Anburaj, G., Marimuthu, M., Sobiyana, P., Manikandan, D.R., 2016. A review on *Tecoma stans*. *Int. J. Eng. Res. Modern Educ.* 1, 2455–4200.
- Dube, E., Oluwale, D.O., Nwaji, N., Nyokong, T., 2018. Glycosylated zinc phthalocyanine-gold nanoparticle conjugates for photodynamic therapy: effect of nanoparticle shape. *Spectrochim. Acta Part A Mol. Biomol. Spectrosc.* 203, 85–95.
- Fatima, N., Kondratyuk, T.P., Park, E.J., Marler, L.E., Jadoon, M., Qazi, M.A., Mehboob Mirza, H., Khan, I., Atiq, N., Chang, L.C., Ahmed, S., Pezzuto, J.M., 2016. Endophytic fungi associated with *Taxus fuana* (West Himalayan Yew) of Pakistan: potential bio-resources for cancer chemo preventive agents. *Pharm. Biol.* 9, 1–8.
- Fu, K.L., Li, X., Ye, J., Lu, L., Xu, X.K., Li, H.L., Zhang, W.D., Shen, Y.H., 2016. Chemical constituents of *Narcissus tazetta* var. chinensis and their antioxidant activities. *Fitoterapia* 113, 110–116.
- Govindappa, M., Sadananda, T.S., Channabasava, R., Vinay, B.R., 2011. *In vitro* anti-inflammatory, lipoxigenase, xanthine Oxidase and acetylcholinesterase inhibitory activity of *Tecoma stans* Juss. *Ex kunth. Int. J. Pharm. Bio-Sci.* 2, 275–285.
- Hammad Aziz, M., Fakhar-E-alam, M., Fatima, M., Shaheen, F., Iqbal, S., Atif, M., Talha, M., Mansoor Ali, S., Afzal, M., Majid, A., Shelih Al Harbi, T., Ismail, M., Wang, Z.M., AlSalhi, M.S., Alahmed, Z.A., 2016. Photodynamic effect of Ni nanotubes on an HeLa cell line. *Public Library Sci. One* 3, 150–295.
- Jain, D., Daima, H.K., Kachnawaha, S., Kothari, S.L., 2009. Synthesis of plant mediated silver nanoparticles using Papaya fruit extract and evaluation of their antimicrobial activities. *Digest J. Nanomater. Biostruct.* 4, 723–772.
- Kaviya, S., Viswanathan, B., 2011. Green synthesis of silver nanoparticles using *Polyalthia longifolia* leaf extract along with D- sorbitol. *J. Nanotechnol.*, 1–5.
- Liu, J., Li, Y., Ren, W., Hu, W.X., 2006. Apoptosis of HL-60 cells induced by extract from *Narcissus tazetta* var. chinensis. *Cancer Lett.* 242, 133–140.
- Luna, C., Chavez, V.H.G., Barriga-Castro, E.D., Nunez, N.O., Mendoza-Resendez, R., 2015. Biosynthesis of silver fine particles and particles decorated with nanoparticles using the extract of *Illicium verum* (star anise) seeds. *Spectrochim. Acta Part A Mol. Biomol. Spectrosc.* 141, 43–50.
- Mafiz, S., Alothman, Z.A., Mohsin, K., 2015. Silver nanoparticles enhanced flow injection chemiluminescence determination of gatifloxacin in pharmaceutical formulation and spiked urine sample. *Spectrochim. Acta Part A Mol. Biomol. Spectrosc.* 144, 170–175.
- Makwana, B.A., Vyas, D.J., Bhatt, K.D., Jani, V.K., Agrawal, Y.K., 2015. Highly stable antibacterial silver nanoparticles as selective fluorescent sensor for Fe<sup>3+</sup> ions. *Spectrochim. Acta Part A Mol. Biomol. Spectrosc.* 134, 73–80.
- Mariselvam, R., Ranjitsingh, J., Nanthini, U.R., Kalirajan, K., Padmalatha, C., Selvakumar, P.M., 2014. Green synthesis of silver nanoparticles from the extract of the inflorescence of *Cocos nucifera* for enhanced antibacterial activity. *Spectrochim. Acta Part A Mol. Biomol. Spectrosc.* 129, 537–541.

- Masood, F., Chen, P., Yasin, T., Fatima, N., Hasan, F., Hameed, A., 2013. Encapsulation of Ellipticine in poly-(3-hydroxybutyrate-co-3-hydroxyvalerate) based nanoparticles and its *in-vitro* application. *Mater. Sci. Eng. C* 33, 1054–1060.
- Mativandela, S., Lall, N., Meyer, J.J.M., 2006. Antibacterial, antifungal and antitubercular activity of (the roots of) *Pelargonium reniforme* (CURT) and *Pelargonium sidoides* (DC) (Geraniaceae) root extracts. *S. Afr. J. Bot.* 72, 232–237.
- Mehrotra, V., Mehrotra, S., Kirar, V., Shyam, R., Misra, K., Srivastava, A.K., Nandi, S., 2017. Antioxidant and antimicrobial activities of aqueous extract of *Withania somnifera* against methicillin-resistant *Staphylococcus aureus*. *Int. J. Microbiol. Biotechnol.* 1, 40–45.
- Nabikhan, A., Kandasamy, K., Raj, A., Alikunhi, N., 2010. Synthesis of antimicrobial silver nanoparticles by callus and leaf extracts from saltmarsh plant, *Sesuvium portulacastrum*. *Colloids Surfaces B: Biointerfaces* 79, 488–493.
- Ogawara, K., Higaki, K., 2017. Nanoparticle-based photodynamic therapy: current status and future application to improve outcomes of cancer treatment. *Chem. Pharm. Bull.* 65, 637–664.
- Samberg, M.E., Oldenburg, S.J., Monteiro-Riviere, N.A., 2011. Evaluation of silver nanoparticles toxicity *in vivo* skin and *in vitro* keratinocytes. *Environ. Health Perspect.* 1, 153–162.
- Tang, R., Habimana-Griffin, M.L., Lane, D.D., Egbulefu, C., Achilefu, S., 2017. Nanophoto sensitive drugs for light-based cancer therapy: what does the future hold. *Nanomedicine (London, England)* 12, 1101–1105.
- Vacik, J.P., Davis, C.L., Kelling, L.J., Schermeister, I.A., 1979. Current status of studies on the antiviral activity of water-soluble extract from *Narcissus* bulb against *herpes virus*. *Adv. Ophthalmol.* 38, 281–287.
- Varadavenkatesan, T., Selvaraj, R., Vinayagam, R., 2019. Green synthesis of silver nanoparticles using *Thunbergia grandiflora* flower extract and its catalytic action in reduction of Congo red dye. *Mater. Today. Proc.* 23, 39–42. <https://doi.org/10.1016/j.matpr.2019.05.441>.
- Varadavenkatesan, T., Pai, S., Vinayagam, R., Selvaraj, R., 2021. Characterization of silver nano-spheres synthesized using the extract of *Arachis hypogaea* nuts and their catalytic potential to degrade dyes. *Mater. Chem. Phys.* 272, <https://doi.org/10.1016/j.matchemphys.2021.125017> 125017.
- Vinayagam, R., Varadavenkatesan, T., Selvaraj, R., 2017. Evaluation of the anticoagulant and catalytic activities of the *Bridelia retusa* fruit extract-functionalized silver nanoparticles. *J. Clust. Sci.* 28, 2919–2932. <https://doi.org/10.1007/s10876-017-1270-5>.